molecular
human
reproduction

ORIGINAL RESEARCH

Cannabis significantly alters DNA methylation of the human ovarian follicle in a concentration-dependent manner

Noga Fuchs Weizman [1,2,†], **Brandon A. Wyse** [1,*,†], **Janice Montbriand**, **Sahar Jahangiri**[1,4], **and Clifford L. Librach**[1,4,5,6]

[1]CReATe Fertility Centre, Toronto, ON, Canada [2]Racine IVF Unit, Lis Maternity Hospital, Tel Aviv Sourasky Medical Center, Affiliated to the Sackler Faculty of Medicine, Tel Aviv University, Tel Aviv, Israel [3]Department of Anesthesia, Sunnybrook Health Sciences Centre, Toronto, ON, Canada [4]CReATe BioBank, Toronto, Canada [5]Department of Obstetrics and Gynecology, University of Toronto, Toronto, ON, Canada [6]Department of Physiology, University of Toronto, Toronto, ON, Canada

*Correspondence address. CReATe Fertility Centre, 790 Bay St. Suite 420, Toronto, ON M5G 1N8, Canada. Tel: +1-416-323-7727; E-mail: brandon@createivf.com;brandonwyse@gmail.com https://orcid.org/0000-0001-9266-1962

ABSTRACT: Cannabis is increasingly consumed by women of childbearing age, and the reproductive and epigenetic effects are unknown. The purpose of this study was to evaluate the potential epigenetic implications of cannabis use on the female ovarian follicle. Whole-genome methylation was assessed in granulosa cells from 14 matched case-control patients. Exposure status was determined by liquid chromatography–mass spectrometry (LC-MS/MS) measurements of five cannabis-derived phytocannabinoids in follicular fluid. DNA methylation was measured using the Illumina TruSeq Methyl Capture EPIC kit. Differential methylation, pathway analysis and correlation analysis were performed. We identified 3679 differentially methylated sites, with two-thirds affecting coding genes. A hotspot region on chromosome 9 was associated with two genomic features, a zinc-finger protein (*ZFP37*) and a long non-coding RNA (*FAM225B*). There were 2214 differentially methylated genomic features, 19 of which have been previously implicated in cannabis-related epigenetic modifications in other organ systems. Pathway analysis revealed enrichment in G protein-coupled receptor signaling, cellular transport, immune response and proliferation. Applying strict criteria, we identified 71 differentially methylated regions, none of which were previously annotated in this context. Finally, correlation analysis revealed 16 unique genomic features affected by cannabis use in a concentration-dependent manner. Of these, the histone methyltransferases *SMYD3* and *ZFP37* were hypomethylated, possibly implicating histone modifications as well. Herein, we provide the first DNA methylation profile of human granulosa cells exposed to cannabis. With cannabis increasingly legalized worldwide, further investigation into the heritability and functional consequences of these effects is critical for clinical consultation and for legalization guidelines.

Key words: cannabis / marijuana / Δ9-THC / DNA methylation / epigenetics / granulosa cells

Introduction

Cannabis, the third most commonly used psychoactive drug by women of childbearing age (Substance Abuse and Mental Health Services Administration (SAMHSA), 2014), has been increasingly legalized worldwide (Smart et al., 2017). This has led, in turn, to increased use across all ages (Rotermann, 2019; Volkow et al., 2019). All cannabis-derived cannabinoids are collectively referred to as phytocannabinoids (PCs). Delta-9-tetrahydrocannabinol (Δ9-THC), the main psychoactive component of cannabis, is used for medicinal and

recreational purposes (Sun and Dey, 2012). Other PCs include cannabidiol (CBD), a non-psychotropic PC that counteracts the psychoactive effects of Δ9-THC, and cannabinol (CBN), a byproduct of Δ9-THC degradation, as well as 11-OH-THC and 11-COOH-THC, both byproducts of Δ9-THC metabolism (ElSohly et al., 2017). Phytocannabinoids exert their actions primarily via two G protein-coupled receptors (GPCRs), cannabinoid receptors 1 and 2 (CB1R and CB2R), by acting as agonists, inverse agonists or as antagonists (Howlett, 2002; Fonseca et al., 2013; Yohn et al., 2015; Brents, 2016). Both receptors can be found in the female reproductive system and

---

are essential for folliculogenesis, oocyte maturation and ovulation, among other reproductive functions (Wang *et al.*, 2006; Taylor *et al.*, 2007; Battista *et al.*, 2008; Maccarrone, 2015; Fuchs Weizman *et al.*, 2021).

Several clinical studies involving self-reported PC use, have shown that exposure to PCs can cause ovulatory abnormalities and impact oocyte quality and pregnancy rates amongst patients undergoing IVF (Mueller *et al.*, 1990; Klonoff-Cohen *et al.*, 2006; Jukic *et al.*, 2007). In our previous study, we reported on measuring PCs in human follicular fluid utilizing liquid chromatography–mass spectrometry (LC-MS/MS), thereby paving the way for objective assessments of the impact of cannabis on female fertility (Fuchs Weizman *et al.*, 2021).

Cannabis exposure can also cause epigenetic modifications, like other environmental agents (Yohn *et al.*, 2015; Szutorisz and Hurd, 2016). It is established that Δ9-THC causes genome-wide histone modifications and altered DNA methylation, in brain, sperm, blood cells and, potentially, the ovarian follicle (Yang *et al.*, 2014; Watson *et al.*, 2015; Yohn *et al.*, 2015; Santoro *et al.*, 2017; Murphy *et al.*, 2018; Levin *et al.*, 2019; Osborne *et al.*, 2020; Schrott *et al.*, 2020; Fuchs Weizman *et al.*, 2021). However, there is still a significant gap in the literature regarding the epigenetic effects of cannabis exposure on the somatic cells supporting oocyte growth and maturation. In our previous study, we showed that PCs alter the epigenetic machinery in human granulosa cells, via decreased expression of DNMT3b, a *de novo* methylating enzyme, which in turn led to decreased global DNA methylation, *in vitro* (Fuchs Weizman *et al.*, 2021). In the current study, we aimed at (i) establishing methylation profiles of naive human granulosa cells, (ii) exploring the effects of cannabis exposure on these profiles and (iii) comparing the epigenetic consequences of cannabis exposure on human granulosa cells to those observed in other cell types.

Materials and methods

Ethical approval

This study received research ethics board (REB) approval (Veritas #16518). All subjects provided written informed consent for the donation of their biological waste material, which included the collection of follicular fluid (FF) and granulosa cells (GC) as well as de-identified clinical information, including age, BMI, ovarian reserve metrics and treatment regimens.

Sample collection

All follicular fluid (FF) samples were obtained from the CReATe Fertility BioBank (Toronto, Canada) which were biobanked from consenting patients undergoing IVF at CReATe Fertility Center (Toronto, Canada), between January 2018 and July 2019. Patients were treated using a standard antagonist protocol, with initial gonadotropin dosing and subsequent adjustments at the discretion of their treating physician. Ultrasound-guided oocyte retrieval was performed ∼36 h following trigger injection. Participants were of similar ethnic background and socioeconomic status, did not report any polysubstance abuse, and all self-identified as 'social drinkers'. The study personnel were blinded to all clinical information pertaining to the tested samples prior to the analysis of PC concentrations.

Measurement of phytocannabinoids in follicular fluid

FF samples were assayed for phytocannabinoid levels (Δ9-THC, 11-OH-THC, 11-COOH-THC, CBD and CBN). FF was utilized to determine if the follicle was a privileged site, determine the concentration of PCs that the oocyte and GCs are exposed to, and (unlike measurement of cannabis in urine) to allow for the measurement of not only metabolites of THC (11-COOH-THC), but the active molecule as well (Δ9-THC). Measurements were performed by LC-MS/MS of the FF at the Analytical Facility for Bioactive Molecule (Hospital for Sick Children, Toronto, Canada) as previously described (Fuchs Weizman *et al.*, 2021).

Inclusion criteria

Seven patients whose FF tested positive for one or more of the PCs were assigned to the case group. These case-patients were matched by demographic (age, BMI and ethnicity) and stimulation parameters (anti-Müllerian hormone, LH on trigger, FSH on Day 2/3 of cycle and E2 on trigger) with seven patients whose samples were negative for all measured PCs (control group). To further reduce inter-patient variability, included patients were of similar ethnic background, with the majority of patients of Caucasian/European descent, while two patients were of South Asian descent, and one patient was of Indigenous descent. No patients reported any recreational drug use, tobacco use, polysubstance use or other medication use during the initial patient intake questionnaire. Polycystic ovary syndrome (PCOS) patients were excluded from this study as PCOS has been shown to alter the methylome of cells in the follicular niche (Xu *et al.*, 2016; Sagvekar *et al.*, 2019). All corresponding granulosa cells (GCs) were retrieved from the CReATe Fertility BioBank (Toronto, Canada).

Sample preparation and DNA extraction

Granulosa cells from all large/dominant follicles were thawed rapidly, using a 37°C water bath, and pooled. Cells were washed in DMEM/F12 + 2.5% Fetal Bovine Serum (FBS) to remove cryoprotectants. The resulting cell pellet was resuspended, and cell number and viability were assessed using the Countess automated cell counter (ThermoFisher Scientific, Mississauga, Canada). Genomic DNA was isolated from ∼50 000 cells using the QIAamp DNA Mini Kit (Qiagen, Hilden, Germany), according to the manufacturer's instructions. Briefly, cells were lysed in Buffer AL and homogenized using a Disruptor Genie for 5 min. The genomic DNA was bound to the supplied column and washed using the supplied buffers. Genomic DNA was eluted in 200 μl of Buffer AE. Total genomic DNA concentration was assayed using the Qubit dsDNA HS Assay (ThermoFisher Scientific, Mississauga, Canada).

Bisulfite sequencing

Samples were sequenced at the Princess Margaret Genomics Centre (Toronto, Canada) using the Illumina TruSeq Methyl Capture EPIC kit (Illumina, Canada), according to the manufacturer's instructions. Briefly, 500 ng of genomic DNA was sheared using a Covaris S220 sonicator (Covaris, MA, USA) to yield fragments of ∼180–220 bp. The fragmented DNA was then end-repaired, poly-A tailed and ligated with uniquely indexed adapters. These indexed libraries were hybridized twice to the EPIC capture oligos to specifically bind regions of

interest. The hybridized probes were captured and purified after each hybridization using streptavidin magnetic beads. The enriched library was bisulfite converted, PCR amplified and purified by magnetic beads. Final libraries were quantified by the Qubit dsDNA HS Assay (Thermo Fisher) and quality was assessed using the 2100 Bioanalyzer High Sensitivity DNA chip (Agilent Technologies, USA). Libraries were normalized and sequenced on a NovaSeq 6000 S2 flow cell (Illumina, Canada) (paired-end 2×100 bp).

Targeted mRNA sequencing

A custom-designed AmpliSeq targeted panel (97 targets total) (Illumina, Canada) was designed to assess the expression of genes whose DNA methylation was either correlated with PC exposure or previously reported to be impacted by PC exposure in other studies. We also included genes that participate in the signaling pathways of cannabinoids including, cannabinoid receptors, DNMTs, GPCR signaling, Zinc homeostasis and other downstream pathways including MAPK, ERK2 and PKA signaling pathways. The 14 samples used for bisulfite sequencing plus an additional 10 samples (7 cases and 3 controls) were subjected to AmpliSeq library preparation according to manufacturer's instructions using the AmpliSeq Library PLUS kit (Illumina, Canada). Final libraries were quantified by the Qubit dsDNA HS Assay (Thermo Fisher) and quality was assessed using the 2100 Bioanalyzer High Sensitivity DNA chip (Agilent Technologies, USA). Libraries were normalized and sequenced on a miSeq v2 flow cell (Illumina, Canada) (paired-end 2×150 bp).

Bioinformatics: differential methylation analysis

FASTQ files were generated using bcl2fastq2 (v2.17) and read quality was assessed using FASTQC (v0.11.8) (Andrews, 2010). Reads were trimmed using trim_galore (v0.5.0) to remove Illumina adapter sequences and low-quality bases (quality = 20, stringency = 7) (Krueger, 2012). The trimmed reads were aligned to Human Genome Assembly 38 (hg38) using bismark (v0.22.1) and bismark_methylation_extractor was used to extract the methylation call for each cytosine base (Krueger and Andrews, 2011). MethylKit (v1.10.0) was used for differential methylation analysis (Akalin et al., 2012). Bases with coverage of <10 in each of the samples were discarded from further analysis. Samples were clustered based on the similarity of their methylation profiles using hierarchical clustering and principal component analysis. CpG were annotated to genic annotations (enhancer, 1–5 kb upstream of the Transcription Start Site (TSS), promoter, exon/3′UTR, intron and intergenic) using the annotation package (v3.12) (Cavalcante and Sartor, 2017). Differentially methylated sites (DMSs) were defined as having a percent methylation difference >25% and an adjusted P-value (q-value) <0.01. Differentially methylated regions (DMRs) were defined as regions of the genome containing at least three CpG with a concordant (either hypo- or hypermethylated) mean methylation difference >25% between cases and controls, within a 1000-bp interval (Watson et al., 2015).

Pathway analysis

Gene set enrichment analysis (GSEA) was conducted on hypo- and hyper-methylated DMS individually, using g:Profiler-g:GOSt (KEGG, Reactome and Wikipathways) with the g:SCS multiple testing correction method, applying a significance threshold of 0.05 (q-value), to determine the effect that all DMS have on cellular processes and functions (Raudvere et al., 2019). Genes that could not be mapped to any gene-set term were excluded from the comparison. Gene sets with fewer than five genes and a q-value >0.05 were excluded from further analysis.

RNA sequencing analysis

Bioinformatics were conducted using Partek Flow. Briefly, reads were trimmed to remove low-quality bases (Phred score < 25), aligned to hg19 using STAR (v2.5.3a) and quantified to the annotation model RefSeq Transcripts 99 (Dobin et al., 2013). Samples were normalized using trimmed mean of M-values (TMM) and differential expression was conducted using DESeq2 comparing cases to controls (Robinson and Oshlack, 2010; Love et al., 2014). Differentially expressed genes were defined as having a fold change (FC) $-2 > FC > 2$ and a false discovery rate <0.05.

Data analysis and literature review

We conducted a literature review of the PubMed database for previous studies assessing the effects of cannabis on DNA methylation in any cell type using a variety of methods (i.e. qPCR, microarray, whole-genome/reduced representation sequencing or targeted sequencing), and cross-referenced the findings with significant DMS within DMR in our analysis. The associated features were further explored in depth using the Ovarian Kaleidoscope Database (Leo and Hsueh, 2000) and GeneCards Human Gene database (http://www.genecards.org/) to correlate our bioinformatic findings with hallmark physiological and pathological processes in the ovary.

Statistical analysis

Mean and SE were utilized for continuous variables. Student's t-test or Fisher's exact tests were used to assess statistical significance. Correlational analysis was used to assess the relationship between PC measures and methylation. Normality was measured using skew and kurtosis, and Pearson or Spearman correlations were used, as appropriate. To control for multiple comparisons, P values from 0.04 to 0.055 were considered a trend, and values below $P = 0.04$ were considered significant. Specific tests used are indicated in all figure and table legends.

Results

Fourteen patients were included in this matched case-control study: seven cases and seven controls. Patient demographics and clinical characteristics are presented in Table I. Cases and controls did not differ significantly in the number of sequencing reads, the number of cytosines analyzed or the average methylation percentage. Overall, there were 3679 DMSs in this study, of which 1741 were hypermethylated, (47.3%) and 1938 were hypomethylated (52.7%) in cases compared with controls. (Supplementary Table SI).

Of all DMS, 497 were in CpG islands (CpGi), 339 were in CpG shores (CpGs) and 2843 were not associated with either CpGi or CpGs (CpG other, CpGo) (Fig. 1A and B) (Supplementary Table SI).

Table I Patient demographics.

	Case (n = 7)	Control (n = 7)	*P*-value
Δ9-THC (nM)	37.7 ± 9.2 (8.1–84.8)	—	—
11-OH-THC (nM)	6.3 ± 1.9 (0–12.3)	—	—
11-COOH-THC (nM)	70.8 ± 16.3 (4.5–143.6)	—	—
Age (years)	31.1 ± 2.0 (23–40)	29.4 ± 1.7 (23–36)	0.554
BMI (kg/m^2)	24.2 ± 1.7 (19–32.6)	26.7 ± 2.2 (20.2–38.4)	0.413
AMH (pmol/l)	20.2 ± 2.0 (14.5–29.6)	23.0 ± 4.1 (11.2–38.6)	0.601
LH on Trigger (IU/ml)	3.0 ± 0.7 (0.7–5.4)	1.9 ± 0.5 (0.3–4.0)	0.307
FSH on Day 2/3 (mIU/ml)	6.7 ± 0.3 (5.7–8.3)	6.0 ± 0.4 (4.7–7.5)	0.291
E2 on Trigger (pmol/l)	10 698.4 ± 2295.0 (6106–24 930)	11 351.0 ± 1350.6 (6279–16 225)	0.853

Data presented as Mean±SEM(Range). THC, Tetrahydrocannabinol; AMH, anti-Müllerian hormone; E2, estradiol; Trigger, day of ovulation trigger.
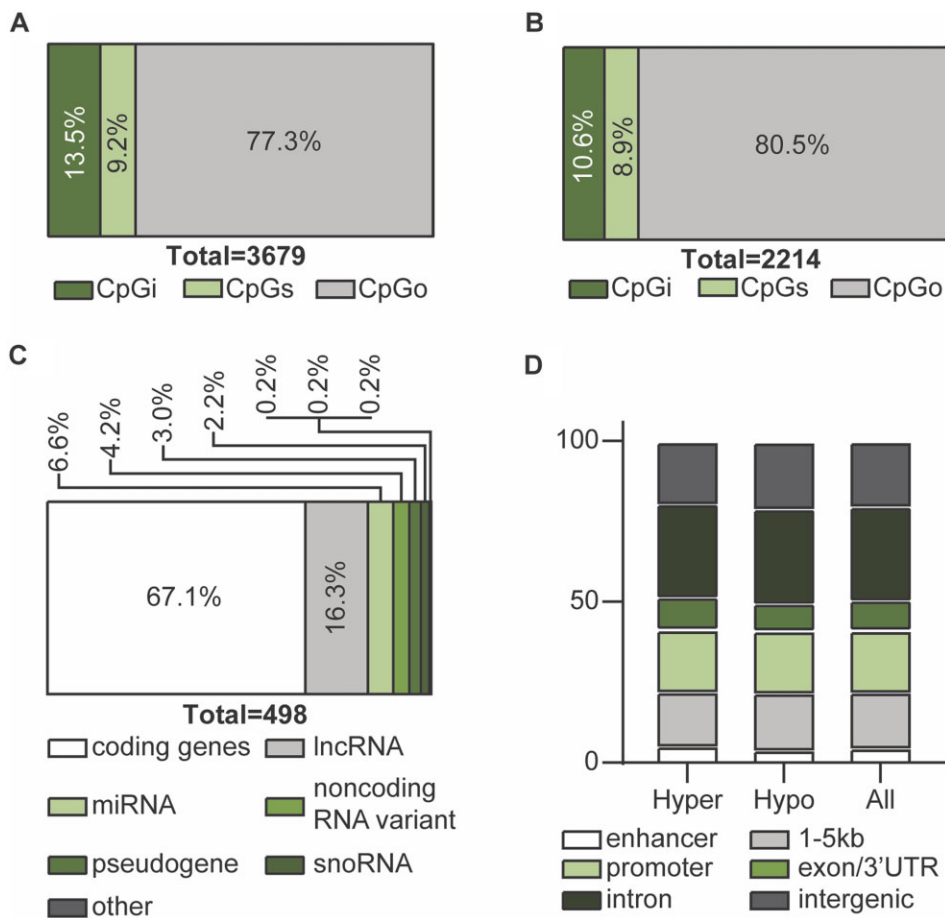
Figure 1. Localization and genomic feature annotation associated with differentially methylated sites (DMS) in case versus control groups. (**A**) Of the 3679 DMS, 497 were associated with CpG islands (CpGi) (13.5%), 339 were associated with CpG shores (CpGs) (9.2%) and 2843 were not associated with either CpGi or CpGs and deemed CpGother (CpGo) (77.3%). (**B**) Of the 2214 unique genomic features that the DMS mapped to, 251 were associated with CpGi (10.6%), 210 were associated with CpGs (8.9%) and 1900 were not associated with either and deemed CpGo (80.5%). (**C**) Stratification of unique genomic feature biotypes of DMS within ±5 kb of the transcription start site. (**D**) Proportions of DMS in hypo-, hyper-methylated and all DMS associated with specific genic annotation using the 'annotatr' package.
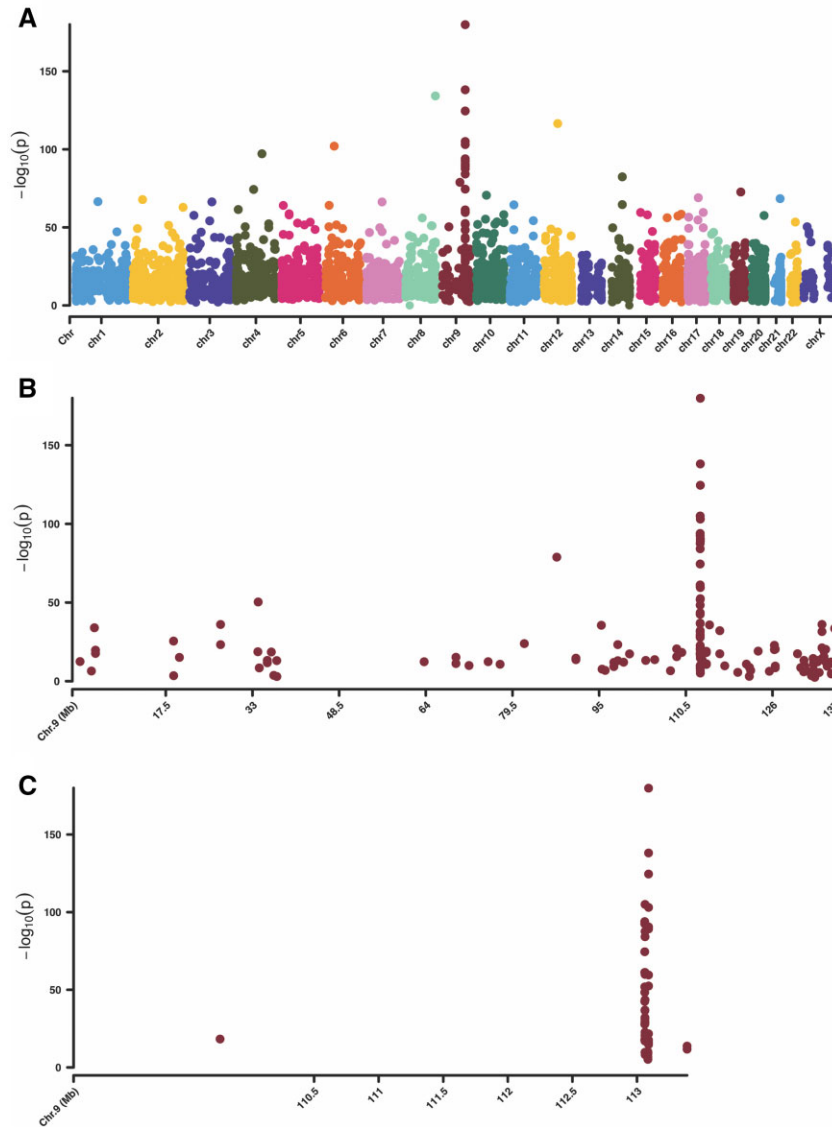
Figure 2. Manhattan plots of the genome-wide differentially methylated sites (DMS) found in the case versus control group. All sites on these plots are significant. Significance is defined as percent methylation difference >25% and an adjusted *P*-value (*q*-value) <0.01. The *y*-axis represents the $-\log_{10}$(adjusted *P*). (**A**) Manhattan plot of all autosomes and the X chromosome. (**B**) Manhattan plot of only chromosome 9, depicting the 'hotspot' region on the distal q arm. (**C**) Manhattan plot of only the chromosome 9 'hotspot' region ranging from chr9:113059999-113089725.

The proportion of DMS, in each of the sublocations, is presented in Fig. 1A, and the proportion of unique genomic features, in the same sublocations, is presented in Fig. 1B. Of DMS within ±5kb of the transcription start site, two-thirds of the features were coding genes, whereas a third were non-coding genes, potentially involved in regulatory functions (Fig. 1C). There was no difference in the distribution of genic annotations between the hypo- and the hyper-methylated DMS (Fig. 1D).

Figure 2A shows a Manhattan plot depicting all CpGs that were identified in this study. A 0.29 Mb region of chromosome 9 (chr9:113059999-113089725) was enriched in DMS (n = 48), driven

by two genomic features; *ZFP37* and the lncRNA *FAM225B* (Fig. 2B and C).

A literature review revealed 19 genomic features (22 DMS) from the current study, which have already been previously annotated in the context of cannabis exposure and epigenetic modifications in human and animal studies exploring its effects in different organ systems (Table II). This study has also identified 2195 differentially methylated features that have not been annotated to date in the context of epigenetic effects attributed to cannabis exposure and are outlined in Supplementary Table SI. Pathway analyses were conducted on the genomic features which were associated with DMS using KEGG,

Table II Differentially methylated sites (DMS) in our study that were also previously reported to be affected by Δ9-THC exposure in other models and organs/systems.

Description	Main function	CpGi % methylation difference	CpGi q value	CpGs % methylation difference	CpGs q value	CpGo % methylation difference	CpGo q value	Species	System	Method	Source
		Current study							**Previous literature**		
TP73 — Tumour protein P73	Tumour suppression	31.67	1.23E−05	—	—	—	—	Human	Blood	EPIC array	Osborne et al. (2020)
ETV2 — ETS variant transcription factor 2	Transcription factor	26.12	1.36E−11	—	—	—	—	Human	Blood	EPIC array	Osborne et al. (2020)
KLHL30 — Kelch like family member 30	Ubiquitin-protein transferase	−45.44	5.92E−29	—	—	—	—	Human and rat	Sperm	RRBS	Murphy et al. (2018)
GAS6-AS1 — GAS6 antisense RNA 1	ncRNA	25.49	1.10E−05	—	—	—	—	Human and rat	Sperm	RRBS	Murphy et al. (2018)
PRKCZ — Protein kinase C zeta	Cellular differentiation and proliferation	26.9	3.22E−05	25.78	3.31E−11	—	—	Rat	Nucleus accumbens	ERRBS	Watson et al. (2015)
PRKCZ — Protein kinase C zeta	Cellular differentiation and proliferation	−38.11	4.36E−15	—	—	—	—	Rat	Nucleus accumbens	ERRBS	Watson et al. (2015)
MGAT3 — Beta-1,4-mannosyl-glycoprotein 4-beta-N-acetylglucosaminyltransferase	Biosynthesis of glycoprotein oligosaccharides	27.21	5.53E−10	—	—	—	—	Rat	Nucleus accumbens	ERRBS	Watson et al. (2015)
LSP1 — Lymphocyte specific protein 1	Regulation of immune cell chemotaxis and adhesion	—	—	−25.08	2.13E−05	44.55	8.48E−30	Rat	Nucleus accumbens	ERRBS	Watson et al. (2015)
ABR — ABR activator of RhoGEF and GTPase	Regulation of macrophage motility and function	—	—	−29.83	8.36E−10	—	—	Rat	Nucleus accumbens	ERRBS	Watson et al. (2015)
KCNMA1 — Potassium calcium-activated channel subfamily M alpha 1	Regulation of smooth muscle tone and neuronal excitability	—	—	−32.17	1.04E−22	—	—	Rat	Nucleus accumbens	ERRBS	Watson et al. (2015)
LZTS2 — Leucine zipper tumour suppressor 2	Tumour suppression	—	—	—	—	−29.95	1.85E−12	Rat	Nucleus accumbens	ERRBS	Watson et al. (2015)
SMYD3 — SET and MYND domain containing 3	Histone methyltransferase	—	—	—	—	−50.22	4.77E−14	Rat	Nucleus accumbens	ERRBS	Watson et al. (2015)
SMYD3 — SET and MYND domain containing 3	Histone methyltransferase	—	—	—	—	−30.58	6.65E−28	Rat	Nucleus accumbens	ERRBS	Watson et al. (2015)
SMYD3 — SET and MYND domain containing 3	Histone methyltransferase	—	—	—	—	−33.76	2.07E−13	Rat	Nucleus accumbens	ERRBS	Watson et al. (2015)
RFC1 — Replication factor C subunit 1	Transcription, DNA replication and repair	—	—	—	—	−27.56	3.72E−10	Rat	Nucleus accumbens	ERRBS	Watson et al. (2015)
ABHD8 — Abhydrolase domain containing 8	Hydrolase activity	—	—	—	—	−27.48	3.31E−17	Rat	Nucleus accumbens	ERRBS	Watson et al. (2015)
GRXCR2 — Glutaredoxin and cysteine rich domain containing 2	Protein S-glutathionylation	—	—	—	—	30.49	1.37E−14	Rat	Nucleus accumbens	ERRBS	Watson et al. (2015)
TOX2 — TOX high mobility group box family member 2	Transcription factor	—	—	—	—	−25.11	1.10E−09	Rat	Nucleus accumbens	ERRBS	Watson et al. (2015)
MFAP2 — Microfibril-associated protein 2	Microfibrils component	—	—	—	—	−31.23	3.21E−09	Rat	Nucleus accumbens	ERRBS	Watson et al. (2015)
EPHA2 — EPH receptor A2	Regulates apoptosis, chemotactic cell migration, adhesion, proliferation, apoptosis and angiogenesis	—	—	—	—	−26.13	4.65E−15	Rat	Nucleus accumbens	ERRBS	Watson et al. (2015)
MPPED1 — Metallophosphoesterase domain containing 1	Metallophosphoesterase	—	—	—	—	25.09	3.56E−17	Rat	Nucleus accumbens	ERRBS	Watson et al. (2015)
AFF3 — AF4/FMR2 family member 3	Transcription factor	—	—	—	—	25.49	1.31E−07	Rat	Nucleus accumbens	ERRBS	Watson et al. (2015)

CpGi, CpG islands; CpGs, CpG shores; CpGo, CpG other (non-island and non-shore); RRBS, reduced-representation bisulfite sequencing; ERRBS, enhanced reduced-representation bisulfite sequencing.
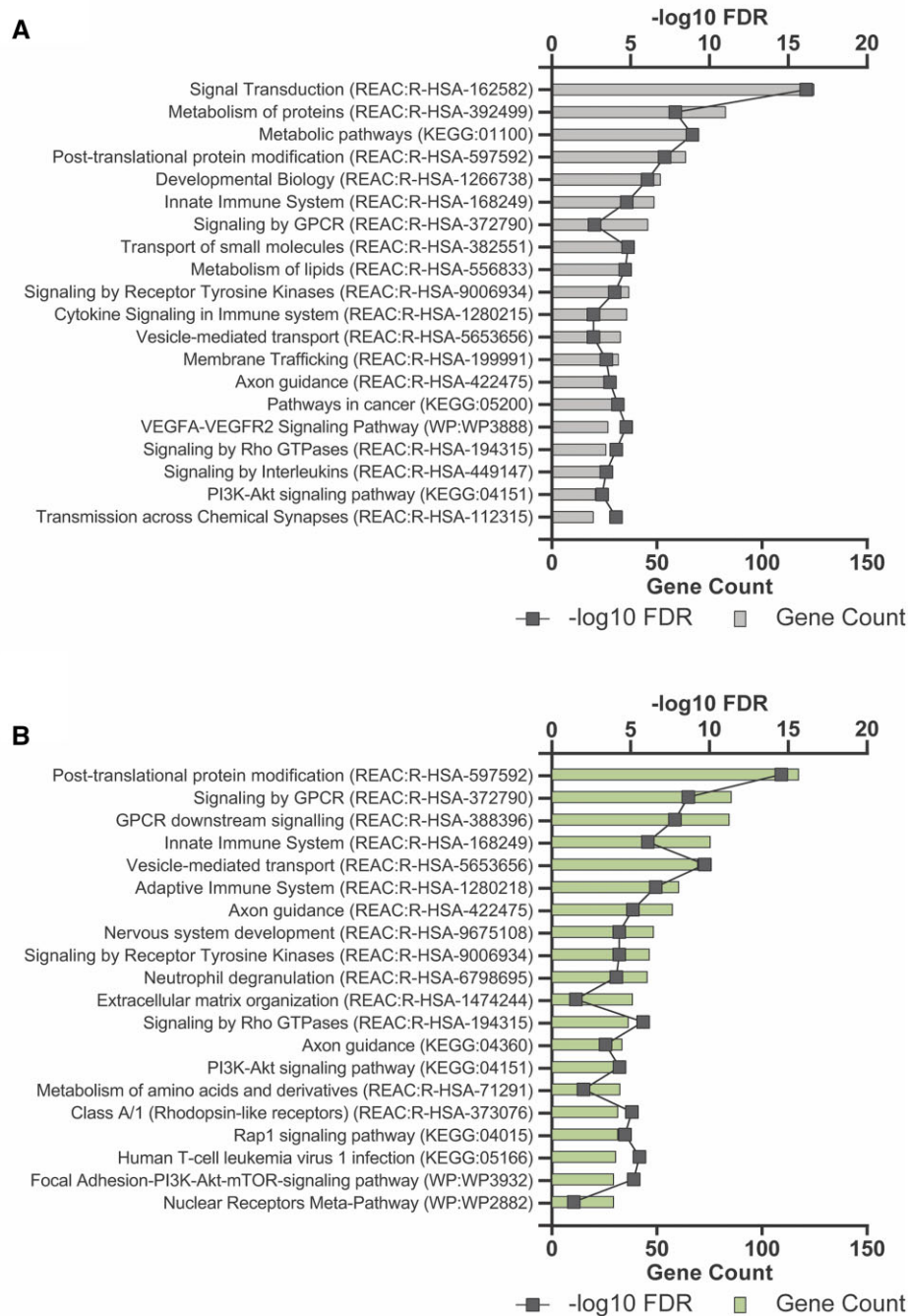
Figure 3. Gene set enrichment analysis of differentially methylated sites (DMS). Gene set enrichment analysis (GSEA) was conducted using g:Profiler-g:GOSt and interrogating KEGG, Reactome and Wikipathways databases. Genesets were considered significant if they had an adjusted *P*-value (*q*-value) <0.05 and five or more genes in the gene set. g:SCS multiple testing correction method was used to determine significance. (**A**) GSEA of all hypomethylated DMS. (**B**) GSEA of all hypermethylated DMS. A full list of gene sets can be found in Supplementary Tables SII and SIII, respectively.

Reactome and Wikipathways using g:Profiler. The hypomethylated DMS (n = 1161) showed enrichment in small molecule transport, innate immune response and developmental biology with the most enriched pathways being involved in signal transduction and metabolism (Fig. 3A, Supplementary Table SII). The hypermethylated DMS (n = 1227) were enriched in similar pathways overall; however, the top pathways were GPCR signaling and immune response (Fig. 3B, Supplementary Table SIII).

In this study, we identified 71 DMR (Supplementary Table SIV). None of the associated features were previously annotated in the context of cannabis exposure and epigenetic modifications. The top 30 DMR are presented in Table III. Of these, 12 are associated with ncRNAs, 6 with enzymes involved in biosynthesis, 5 with regulatory proteins, 4 with adhesion molecules and 3 are associated with genes encoding zinc finger proteins.

To investigate whether there is a concentration-dependent effect of cannabis, we correlated the concentration of either Δ9-THC or 11-COOH-THC in the case group, with the % methylation of all DMS (n = 421) within DMR identified in this study (n = 71), and with features that were previously reported to be affected by cannabis (n = 19). We identified 25 DMS which correlated with Δ9-THC levels (18 were significant, $P < 0.04$; 7 were trending, $0.055 > P > 0.04$), and 16 DMS that correlated with 11-COOH-THC levels (14 were significant, $P < 0.04$; 2 were trending, $0.055 > P > 0.04$). Together, these DMS correspond to 16 unique genomic features (Table IV), some of which had multiple significantly correlated DMS (*FTCD*, *MLLT10P1* and *ZFP37*). Figure 4 depicts examples of four genes that were found to be differentially methylated in a concentration-dependent manner.

Finally, to determine if there is an effect of cannabis on the transcription of genes differentially methylated in this study, genes previously reported to be affected by cannabis exposure in other tissues, or genes involved in downstream signaling in response to cannabis exposure, we performed targeted RNA sequencing (RNASeq) on 97 genes of interest. Of these, 82 genes were detected, and 10 were differentially expressed between cases and controls (8 downregulated, and 2 upregulated). Of note, the promoters of both upregulated genes (*LSP1* and *ZFP57*) were significantly hypomethylated in the cases, and promoters of four downregulated genes (*FTCD*, *KRTAP5-11*, *MGAT3* and *RMRP*) were significantly hypermethylated in the cases. Two genes critical for GC function, *AMH* and *CYP19A1*, were significantly downregulated, -3.10 and -2.11, respectively. Neither of these genes were differentially methylated in this study. We did not detect any alterations to the expression of genes involved in GPCR signaling or the downstream ERK1/2 or AKT signaling pathways. *PRKACG*, a component of the PKA signaling pathway, was significantly downregulated in cases when compared with the control samples, however, this gene was not identified as differentially methylated in this study (Fig. 5 and Supplementary Table SV).

Discussion

Cannabis-related research led to the discovery of the endocannabinoid system (Maccarone, 2015). It is well established that endocannabinoids are important for reproduction-related functions in both males and females (Wang *et al.*, 2006; Taylor *et al.*, 2007; Battista *et al.*, 2015; Maccarone, 2015). The question of whether the presence of phytocannabinoids (cannabis derivatives) disrupt the reproductive functions of endocannabinoids, remains unanswered. However, it has been shown in non-human models and human studies that phytocannabinoids can exert epigenetic effects (Yang *et al.*, 2014; Watson *et al.*, 2015; Yohn *et al.*, 2015; Santoro *et al.*, 2017; Murphy *et al.*, 2018; Levin *et al.*, 2019; Osborne *et al.*, 2020; Schrott *et al.*, 2020; Fuchs Weizman *et al.*, 2021). With increased legalization of cannabis worldwide, cannabis use is on the rise, as previously reported (Rotermann,

2019; Fuchs Weizman *et al.*, 2021). Hence, this study was conducted to explore the potential epigenetic effects of phytocannabinoids (PCs) on the human follicular environment surrounding the growing oocyte.

Herein, we provide the first comprehensive DNA methylation profile of human granulosa cells from patients who have used cannabis and investigate how phytocannabinoids affect DNA methylation. We measured follicular fluid PC concentrations to better understand the effect that PCs have on the immediate environment of granulosa cells and the resulting changes to the methylome of these cells. This study utilized biobanked samples, and as such, data regarding the actual amount of cannabis used was not available and data regarding concomitant drug or medication exposure was limited. It has been established that the pharmacokinetics of PCs are affected by mode of ingestion, and reflect the time that has passed from ingestion, and we have previously elaborated on this topic (Fuchs Weizman *et al.*, 2021). The presence of Δ9-THC in the FF in most patients indicates recent exposure to cannabis (within 24–48 h) as levels in the plasma drop below the limit of detection following this time (Skopp *et al.*, 2003; Balikova *et al.*, 2014). By measuring FF-PC concentrations, we were able to bypass the above hurdles and highlight the effect this concentration has on the methylome of the immediate environment of the follicular niche.

By virtue of our matched case-control study design, we were able to minimize the biologic variability that could potentially affect the epigenome in question. Furthermore, since PCOS is the only condition that has been shown, to date, to affect the follicular niche methylome we chose to exclude PCOS patients from this dataset to control for the confounding effects this diagnosis may have (Xu *et al.*, 2016; Sagvekar *et al.*, 2019).

Of the differentially methylated sites (DMS) in this study, 47% were hypermethylated and 53% were hypomethylated, similarly to a previous report (Watson *et al.*, 2015). There was no difference in the distribution of genic annotations between hypo- and hyper-methylated DMS, with the largest proportion being either within a confirmed promoter or within a predicted promoter (within 5 kb of the TSS), followed by DMS located in the introns and then intergenic genes. Two-thirds of affected features were coding genes, whereas a third were non-coding regions and potentially involved in regulatory functions.

A striking feature of our bioinformatic analysis was a 'hotspot' of differential methylation in a 0.29 Mb region on chromosome 9, which was enriched in 48 DMS. Looking closely, we observed the region to be highly dense with CpGi. This, in turn, affected two genomic features, the zinc finger protein *ZFP37*, and the long non-coding RNA (lncRNA), *FAM225B*. *ZFP37* is known to be highly expressed in the ovary, second only to its expression in the central nervous system (GTEx Consortium, 2013). In their study, Watson *et al.* (2015) found eight different ZFPs to be differentially methylated in the rat nucleus accumbens following exposure to Δ9-THC, and ZFPs were also in their top five DMR enrichment analysis. In mice *ZFP37* has been identified as a transcript that is enriched in growing/developing follicles and may be a marker of oocyte potential, however its mechanism of action and specific targets have yet to be elucidated (Herrera *et al.*, 2005). Furthermore, the KRAB-ZFP family, of which *ZFP37* is a member, has been proposed to mediate histone deacetylation and H3-K9 trimethylation (H3-K9-me3) through the formation of a potent epigenetic silencing complex with KAP1. This complex recruits histone deacetylases and methyltransferases, resulting in the formation of

Table III The top 30 differentially methylated regions (DMR).

Location	DMR state	Size (bp)	Significant CpG	q value	Mean % methylation difference	Max % methylation difference	Genomic feature	Description	Main function	annotar Genic annotation
chr10:1097887-1098690	Hypo	803	3	6.21E−38	−50.42	−53.77	IDI1	Isopentenyl-diphosphate delta isomerase 1	Cholesterol synthesis	Intron
chr12:32792786-32792901	Hypo	115	4	3.85E−30	−52.45	−56.30	YARS2	Tyrosyl-TRNA synthetase 2	Mitochondrial translation	Exon and promoter
chr10:133286049-133286495	Hyper	446	3	8.07E−29	31.55	35.37	ADAM8	ADAM metallopeptidase domain 8	Adhesion	1 to 5 kb
chrX:115888618-115888639	Hyper	21	5	3.20E−26	28.49	36.23	DANT1	DXZ4-associated non-coding transcript 1, proximal	ncRNA	Intron
chr19:52596457-52596505	Hypo	48	3	1.26E−23	−39.64	−43.79	ZNF137P	Zinc finger protein 137, pseudogene	ncRNA	Exon
chr9:134838539-134839110	Hypo	571	3	2.16E−22	−38.96	−43.99	MIR3689C	MicroRNA 3689c	ncRNA	Intron
chr10:80450825-80450885	Hypo	60	3	4.37E−20	−36.08	−37.80	TSPAN14	Tetraspanin 14	Innate immunity-MMP trafficking	1 to 5 kb
chr9:113059999-113060198	Hypo	199	9	1.84E−19	−28.01	−33.12	ZFP37	ZFP37 zinc finger protein	Zinc-finger	1 to 5 kb
chr11:71587803-71588521	Hyper	718	3	3.19E−19	34.87	37.96	KRTAP5-11	Keratin-associated protein 5-11	Adhesion	1 to 5 kb
chr9:113061674-113061745	Hypo	71	8	1.26E−18	−33.09	−41.29	ZFP37	ZFP37 zinc finger protein	Zinc-finger	1 to 5 kb
chr18:112336-112400	Hypo	64	4	1.08E−17	−26.71	−28.20	MIR8078	MicroRNA 8078	ncRNA	Promoter
chr20:61389938-61390521	Hyper	583	3	3.83E−17	35.53	37.18	CDH4	Cadherin 4	Adhesion	Intron
chr20:56987407-56988020	Hypo	613	3	8.94E−17	−33.66	−35.22	BMP7-AS1	BMP7 antisense RNA 1	ncRNA	Intergenic
chr9:113089352-113089725	Hypo	373	12	1.68E−16	−28.25	−33.86	FAM225B	Family with sequence similarity 225 member B	ncRNA	1 to 5 kb
chr4:2399815-2400293	Hypo	478	5	1.81E−16	−29.51	−34.68	ZFYVE28	Zinc finger FYVE-type containing 28	EGFR signaling	Intron
chrX:126472512-126472534	Hypo	22	4	2.48E−16	−41.81	−44.40	DCAF12L1	DDB1 and CUL4-associated factor 12 like 1	Protein complex formation	Enhancer
chr4:521699-522056	Hyper	357	3	5.34E−16	31.90	33.03	PIGG	Phosphatidylinositol glycan anchor biosynthesis class G	Post-translational modification	Promoter
chr2:130037205-130038141	Hypo	936	6	4.38E−15	−29.68	−36.44	FAR2P1	Fatty Acyl-CoA reductase 2 pseudogene 1	ncRNA	1 to 5 kb
chr5:160186362-160186495	Hyper	133	3	5.50E−15	40.74	46.77	FABP6	Fatty acid binding protein 6	Bile synthesis	Promoter
chr2:241666232-241666548	Hyper	316	3	3.57E−14	38.93	44.52	DTYMK	Deoxythymidylate kinase	Pyrimidine synthesis	Promoter
chr8:134466004-134466775	Hyper	771	3	2.92E−13	31.49	34.94	ZFAT-AS1	ZFAT antisense RNA 1	ncRNA	Intergenic
chr4:1050997-1051032	Hyper	35	3	3.14E−13	26.54	27.11	FGFRL1	Fibroblast growth factor receptor like 1	Cell proliferation	Intergenic
chr6:52995723-52995825	Hyper	102	12	6.59E−13	34.20	39.77	RN7SK	RNA component of 7SK nuclear ribonucleoprotein	ncRNA	Promoter

(continued)

Table III Continued

| Location	DMR state	Size (bp)	Significant CpG	q value	Mean % methylation difference	Max % methylation difference	Genomic feature	Description	Main function	Genic annotation
chr9:35657904-35657916	Hyper	12	3	1.26E-12	28.11	29.91	RMRP	RNA component of mitochondrial RNA processing endoribonuclease	Mitochondrial RNA processing	Promoter
chr20:63074755-63075677	Hypo	922	4	1.87E-12	-37.56	-42.54	HAR1A	Highly accelerated region 1A	ncRNA	Intron
chr4:536425-537351	Hyper	926	3	2.47E-12	33.85	44.09	PIGG	Phosphatidylinositol glycan anchor biosynthesis class G	Post-translational modification	Exon
chr17:3981605-3981676	Hypo	71	4	5.95E-12	-40.27	-49.37	LINC01975	Long intergenic non-protein coding RNA 1975	ncRNA	Exon
chr12:131434953-131435002	Hyper	49	4	1.38E-11	35.30	36.11	LINC02370	Long intergenic non-protein coding RNA 2370	ncRNA	1 to 5 kb
chr9:113062049-113062461	Hypo	412	12	1.48E-11	-28.54	-34.96	ZFP37	ZFP37 zinc finger protein	Zinc-finger	1 to 5 kb
chr17:7148150-7148200	Hypo	50	4	2.28E-11	-35.39	-41.17	ASGR1	Asialoglycoprotein receptor 1	Glycoprotein homeostasis	Intergenic

heterochromatin and repression of genes expression. KRAB-ZFPs have been implicated in several biological processes in humans, including protection of imprinting control regions in mice and human embryonic stem cells (hESC) (Juan and Bartolomei, 2019; Takahashi et al., 2019), retroelement silencing in hESC (Rowe et al., 2010; Pontis et al., 2019), and carcinogenesis (Machnik et al., 2019; Cylwa et al., 2020; Sobocinska et al., 2021). Notably, Juknat et al. (2012) suggested that cannabis affects zinc homeostasis which could potentially explain the antioxidant and anti-inflammatory effects of CBD and, to a lesser extent, that of Δ9-THC. Further investigation into *ZFP37* and other ZPFs identified in this study is ongoing, specifically with the aim to identify their binding partners and the genomic features they are associated with. This information will be the first step in understanding their mode of action in GCs and how cannabis may be altering their function.

FAM225B belongs to the lncRNA family and, as such, it is difficult to predict by which mechanism it exerts its regulatory function (Yang et al., 2016). However, previous studies have shown it to be involved in Wnt signaling and cell cycle regulation (Li et al., 2020). Our findings point to the need for further exploration of this potentially enhanced sensitivity of ZFPs and lncRNAs to epigenetic changes caused by cannabis derivatives.

Of all differentially methylated genomic features identified in the current study, 19 have been previously annotated in the context of cannabis exposure and epigenetic modifications. Of these, four either activate transcription or support it (*AFF3*, *ETV2*, *RFC1* and *TOX2*), four regulate cell proliferation and apoptosis (EPHA2, *LZTS2*, *PRKCZ* and *TP73*), three are involved in post-translational modifications (GRXCR2, *KLHL30* and *MGAT3*), and three are involved in extracellular matrix remodeling (ABHD8, *MFAP2* and *MPPED*) (Table II). Notably, two exert their actions primarily in immune cells (*ABR* and *LSP1*) and one is a histone methyltransferase (*SMYD3*) (Table II). Interestingly, we were also able to demonstrate a concentration-related effect of cannabis on three of the differentially methylated genomic features from our study that were annotated previously in the context of cannabis-associated DNA differential methylation: *ABR*, known to regulate macrophage actions, was negatively correlated with Δ9-THC concentration; *KCNMA1*, which encodes for a subunit of potassium channels and plays a key role in controlling excitability in several systems, was positively correlated with Δ9-THC concentration; and *SMYD3*, which associates with the RNA polymerase complex, was negatively correlated with Δ9-THC concentrations. *SMYD3* is a histone methyltransferase, and plays an important role in transcriptional activation. In bovine oocytes, *SMYD3* has been shown to regulate transcription during oocyte maturation and early embryonic development (Bai et al., 2016). In fact, the knockdown of *SMYD3* expression in GV oocytes causes a significant reduction in *NANOG* expression resulting in embryos arresting at the 4- to 8-cell stage (Bai et al., 2016). Furthermore, SMYD3 targets not only histones (H3-K4, H4-K5 and H2A.Z.1-K101), but non-histone proteins as well (VEGFR1, MAP3K2, AKT1 and HER2) which, in turn, stimulate angiogenesis and cell growth and survival and are implicated in carcinogenesis (Bottino et al., 2020). Importantly, this is the second gene, along with *ZFP37*, capable of either directly or indirectly altering histone acetylation/methylation, further implicating cannabis exposure in histone modification alterations in addition to changes in DNA methylation patterns. Further investigation into the impact cannabis has on histone modifications is ongoing.

Table IV Correlation with phytocannabinoids (PC) concentration and DNA methylation.

| Location	Feature name	Family	Function	Identified in previous study	THC correlation coefficient	P value	THC-COOH correlation coefficient	P value
chr17:1028783	ABR	Rho family of GTP-binding proteins	Regulates neuronal and macro-phage activity	Yes	−0.807	0.03	−0.807	0.03
chrX:126472512	DCAF12L1	WD repeat protein family	Coordinating multi-protein complex assemblies	No	−0.821	0.02	−	−
chr1:232142881	DISC1-IT1	lncRNA	Unknown	No	−0.818	0.03	−	−
chr21:46161446	FTCD	Transferase enzyme	Folate-dependent enzyme	No	−	−	0.760	0.05
chr21:46161478	FTCD	Transferase enzyme	Folate-dependent enzyme	No	−	−	0.794	0.03
chr21:46161584	FTCD	Transferase enzyme	Folate-dependent enzyme	No	0.793	0.03	0.803	0.03
chr21:46161499	FTCD	Transferase enzyme	Folate-dependent enzyme	No	0.881	0.01	0.847	0.02
chr21:46161497	FTCD	Transferase enzyme	Folate-dependent enzyme	No	0.858	0.01	0.902	0.01
chr21:46161492	FTCD	Transferase enzyme	Folate-dependent enzyme	No	0.870	0.01	0.930	0.002
chr21:46161556	FTCD	Transferase enzyme	Folate-dependent enzyme	No	0.903	0.01	0.961	0.001
chr21:46161714	FTCD	Transferase enzyme	Folate-dependent enzyme	No	0.648	0.01	−	−
chr21:46161540	FTCD	Transferase enzyme	Folate-dependent enzyme	No	0.745	0.06	−	−
chr21:46161526	FTCD	Transferase enzyme	Folate-dependent enzyme	No	0.746	0.05	−	−
chr21:46161528	FTCD	Transferase enzyme	Folate-dependent enzyme	No	0.781	0.04	−	−
chr21:46161115	FTCD	Transferase enzyme	Folate-dependent enzyme	No	0.784	0.04	−	−
chr10:77640334	KCNMA1	Ion channel	Control of smooth muscle tone	Yes	−	−	0.785	0.04
chr12:52317764	KRT83	Keratin gene family	Structural molecule	No	−0.859	0.01	−0.903	0.01
chr22:50085800	MLC1	Predicted integral membrane transporter	Unknown	No	−	−	−0.792	0.03
chr20:30585672	MLLT10P1	Pseudogene	Unknown	No	−0.753	0.05	−0.881	0.03
chr20:30585291	MLLT10P1	Pseudogene	Unknown	No	−	−	−0.750	0.05
chr20:30586485	MLLT10P1	Pseudogene	Unknown	No	−0.809	0.03	−	−
chr21:32300477	MRAP	MRAP family	Signaling in response to corticotropin	No	−0.867	0.01	−	−
chr4:534708	PIGG	Transferase enzyme	post translational modification	No	−0.764	0.05	−	−
chr1:246417416	SMYD3	Histone methyltransferase	H3K4 di- and tri- methylation	Yes	−0.821	0.02	−	−
chr21:46185079	SPATC1L	Speriolin family	Centrosome component	No	−0.757	0.05	−	−
chr2:94871757	TEKT4	Tektin family	Structural component of the flagellum	No	−	−	0.783	0.04
chr3:194598761	TMEM44-AS1	lncRNA	Unknown	No	0.849	0.02	0.894	0.01
chr8:134466775	ZFAT-AS1	lncRNA	Unknown	No	0.929	0.003	0.929	0.003
chr9:113062448	ZFP37	Zinc finger	Transcriptional regulation	No	−0.788	0.04	−	−
chr9:113062240	ZFP37	Zinc finger	Transcriptional regulation	No	−0.786	0.04	−	−
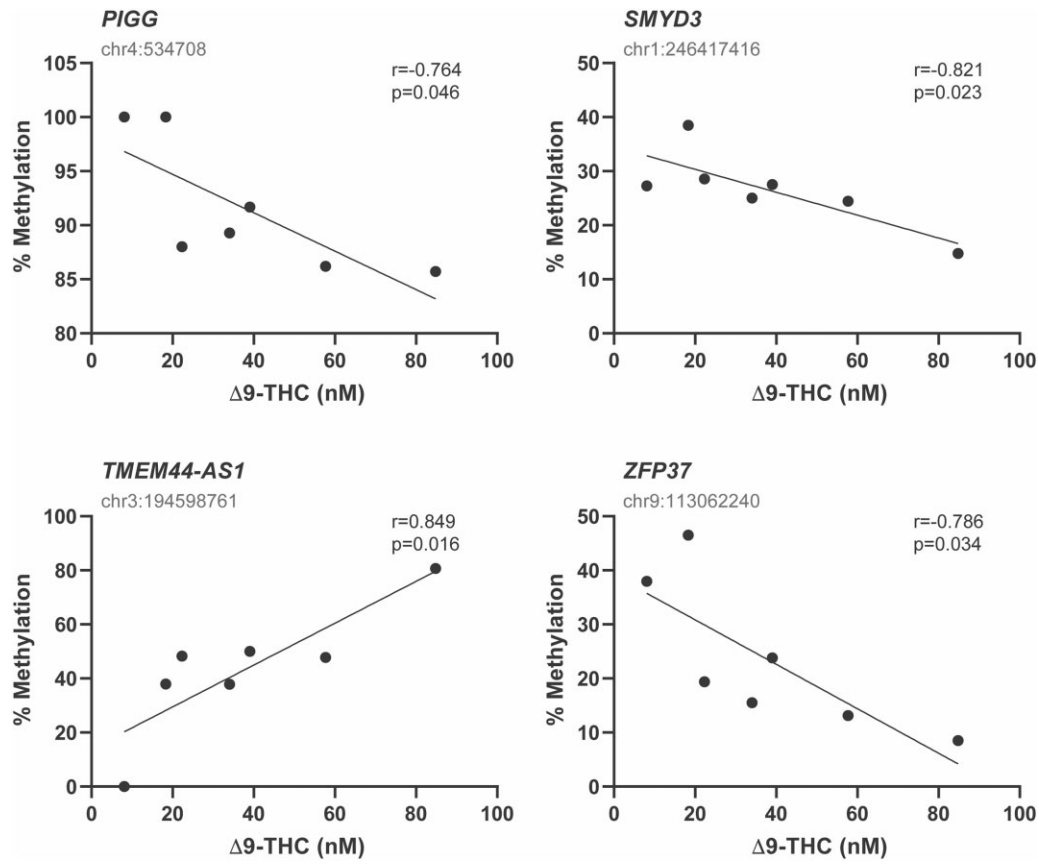
Figure 4. Correlation analysis of differentially methylated regions (DMR) and cannabis usage. Correlations between follicular fluid Δ9-THC concentration in the cannabis group and granulosa cell DNA methylation levels for DMS identified as differentially methylated, analyzed by Pearson correlation. To control for multiple comparisons, *P* values from 0.04 to 0.055 were considered a trend, and values below $P = 0.04$ were considered significant. All DMS displaying a concentration-dependent effect can be found in Table IV.

The current study also identified 2195 novel DMS, in the context of cannabis and epigenetic modifications, which adds significantly to the existing literature and supports future research. Pathway analyses, based on these DMS, portrayed enrichment in cell signaling and metabolism amongst hypomethylated sites, and enriched GPCR signaling and immune response amongst hypermethylated sites. The pathways enriched in DMS are consistent with previous literature investigating the effect cannabis has on the sperm methylome including Hippo signaling, pathways in cancer and MAPK signaling (Murphy et al., 2018).

To elaborate on a key pathway identified, we observed significant hypermethylation of genomic features involved in GPCR signaling. Phytocannabinoids and endocannabinoids exert their effects through GPCRs, namely CB1R and CB2R (Howlett, 2002; Fonseca et al., 2013; Yohn et al., 2015; Brents, 2016). Cecconi et al. (2019) have established that blocking these receptors causes cAMP levels to drop and prevents meiotic resumption in mouse oocytes. Treinen et al. (1993) achieved similar results in a rat model, by competitive inhibition of these receptors with in vitro Δ9-THC treatment. To date, there have

been two studies assessing the effect of in vitro Δ9-THC treatment on bovine oocyte maturation, yielding conflicting results (Lopez-Cardona et al., 2016; Misner et al., 2021). Based on our findings and previous literature, we hypothesize that the hypermethylation of genes involved in GPCR signaling in response to cannabis exposure, and the reduced transcription that may ensue, represent a cellular response mechanism to protect the cell from overstimulation of the GPCR cascade, thereby rescuing meiotic resumption of the oocyte. Hence, further research is needed to determine the effect cannabis has on human oocyte maturation and ART outcomes.

To focus our analysis, and minimize the inclusion of false-positive CpG, we defined a sliding window of 1000-bp containing at least three CpG with a concordant mean methylation difference >25% and a *q*-value < 0.01, as being a differentially methylated region (DMR), as previously described (Watson et al., 2015). After applying these criteria, we identified 71 DMRs of which, within the top 30, there was representation of ZFP family, as well as genomic features involved in adhesion (*ADAM8, KRTAP5-11, CDH4*), biosynthesis (*IDI1, FABP6, DTYMK,*
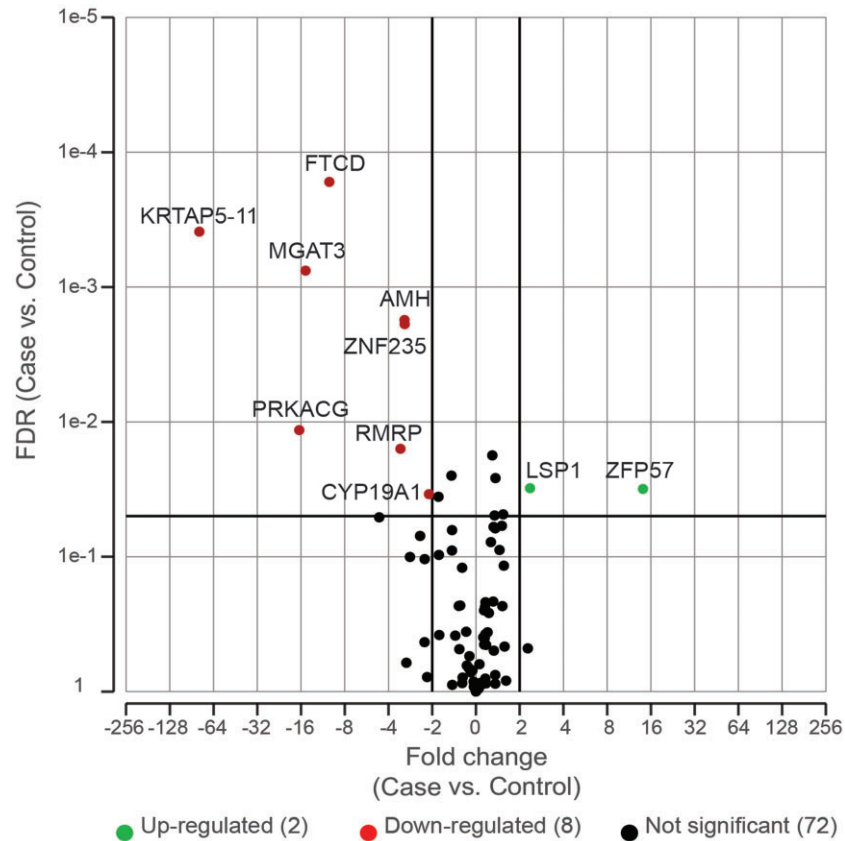
Figure 5. Volcano plot of targeted RNASeq of cases versus controls. Target RNAseq was conducted on 24 samples (14 cases and 10 controls) using a custom designed ampliseq target panel. Differential expression was conducted using DESeq2. Genes were considered differentially expressed with a fold change (FC) $2 < FC < -2$.

ASGR1), translation and post-translational modifications (*YARS2*, *PIGG*, *RMRP*) (Table III). Once again, there was a significant representation of ncRNAs which may have regulatory functions.

Next, we explored the concentration-related effects of cannabis on DNA methylation. For the purpose of this analysis, we focused on genomic features that are a part of a DMR in the current study, as well as on genomic features which were previously annotated in the context of epigenetic effects of cannabis exposure. Together, there were 16 unique genomic features that exhibited concentration-related differential methylation (Table IV), three of which have been previously annotated as affected by exposure to cannabis (*ABR*, *KCNMA1* and *SMYD3*). Interestingly, these 16 genomic features participate in diverse cellular processes including GTP hydrolysis (*ABR*), folate pool regulation (*FTCD*), voltage-gated potassium channel activity (*KCNMA1*), structural cellular components (*DCAF12L1*, *KRT83*, *MLC1*, *SPATC1L* and *TEKT4*), steroid synthesis (*MRAP*), chromatin regulation (*SMYD3*), non-coding RNAs (*DISC1-IT1*, *MLLT10P1*, *TMEM44-AS1* and *ZFAT-AS1*) and transcription regulation (*PIGG* and *ZFP37*).

Finally, to determine the impact cannabis exposure has on hallmark genes and pathways by changing their methylation, we assessed the transcription of 97 genes of interest which were chosen because they were differentially methylated in this study, previously reported to be affected by cannabis use in other tissues, or involved in downstream signaling in response to cannabis exposure. Of these genes, 10 were differentially expressed between cases and controls (2 upregulated and 8 downregulated). Interestingly, the promoters of both upregulated genes (*LSP1* and *ZFP57*) were significantly hypomethylated, and those of four downregulated genes (*FTCD*, *KRTAP5-11*, *MGAT3* and *RMRP*) were significantly hypermethylated in this study, indicating that DNA methylation is altered by cannabis exposure and this is translated into transcriptional changes. Interestingly, in the brain, chronic exposure to cannabis has been shown to decrease PKA activity (Kesner and Lovinger, 2021). PKA signaling is involved in numerous functions including glucose and lipid metabolism, transcription factor regulation, cell adhesion and calcium homeostasis, and alterations to its transcription or activity can have significant downstream effects (Sassone-Corsi, 2012). In this study, we observed decreased expression of a catalytic subunit of PKA (*PRKACG*) in patients who had used cannabis when compared to those who had not, however this downregulation was not caused by alterations in DNA methylation. The decrease in expression is likely in response to cannabis through signaling via the CBRs and downstream GPCRs, much like that observed in the brain (Kesner and Lovinger, 2021). Further exploration of the functional impact of these genes, other potential mechanisms of action, as well as a

larger impact on transcription in the context of oocyte development and folliculogenesis is ongoing. Finally, two genes critical to granulosa cell function, *AMH* and *CYP19A1*, were significantly downregulated in patients who used cannabis compared to controls; however, there were no observed changes to DNA methylation in either of these genes, indicating that cannabis alters the expression of these genes through a DNA methylation-independent mechanism (Fig. 5).

Our study is limited by the probe-based enrichment method we employed because it tends to enrich CpG associated with a higher CpG density, and may miss CpG associated with less dense CpG regions. Furthermore, since the present study was cross-sectional in design, we do not know how exposure over time, frequency of exposure, route of exposure (inhalation or ingestion) or type of cannabis product consumed (flower, oil or refined product) might influence the methylome. However, by establishing correlations between methylome alterations and FF concentrations of PCs, we were able to strengthen our findings and eliminate the bias that may have been introduced by all the above. In addition, FF was not measured for the presence of other psychoactive drugs, and even though none of the patients reported concomitant tobacco use or the use of other psychoactive drugs or prescription medications, self-reporting alone cannot rule out the exposure of the follicle to these substances, and this is a limitation of our study. This study is also limited by its small sample size; however, by matching case and control patients by several confounding variables, we were able to minimize the inter-patient variability. This study was not designed, and was hence underpowered, to determine the effect cannabis exposure has on IVF outcomes. Finally, this study was not designed to examine the reversibility of the epigenetic modifications or their functional consequences. To further our understanding of the functional effects of cannabis on the developing oocyte, as well as the impact on IVF outcomes, we are currently conducting a larger scale study.

Conclusions

To our knowledge, this is the first study profiling the methylome of human granulosa cells exposed to cannabis. We have described key genes involved in GPCR signaling, cell proliferation, apoptosis, immune response, metabolism and histone modifications that were affected. Moreover, we have characterized a concentration-dependent relationship between cannabis concentration and DNA methylation as well as alterations to gene expression directly related to changes in DNA methylation. As cannabis legalization increases worldwide and with its use increasing in women of reproductive age, it is critical that we expand our understanding of the effects cannabis has on the developing ovarian follicle and the oocyte itself. If future studies point to the heritability and functional consequences of these epigenetic modifications, these findings must be considered for drafting cannabis policy decisions, for public education, and for consulting patients.

Supplementary data

Supplementary data are available at *Molecular Human Reproduction* online.

Data availability

The data underlying this article are available in the article and in its online supplementary material. Raw sequencing data can be made available by contacting the corresponding author.

Authors' roles

N.F.W., B.A.W. and C.L.L. designed this study. N.F.W. and B.A.W. analyzed the data, interpreted the results and drafted the manuscript. B.A.W. performed the experiments. J.M. performed the statistical analysis. S.J. collected, processed and released samples and de-identified clinical data. All authors read and approved the final version of the paper.

Conflict of interest

The authors declare no conflicts of interest.

References

Akalin A, Kormaksson M, Li S, Garrett-Bakelman FE, Figueroa ME, Melnick A, Mason CE. methylKit: a comprehensive R package for the analysis of genome-wide DNA methylation profiles. *Genome Biol* 2012;**13**:R87.

Andrews S. FastQC: a quality control tool for high throughput sequence data. 2010. https://www.bioinformatics.babraham.ac.uk/projects/fastqc/ (November 2020, date last accessed).

Bai H, Li Y, Gao H, Dong Y, Han P, Yu H. Histone methyltransferase SMYD3 regulates the expression of transcriptional factors during bovine oocyte maturation and early embryonic development. *Cytotechnology* 2016;**68**:849–859.

Balikova M, Hlozek T, Palenicek T, Tyls F, Viktorinova M, Melicher T, Androvicova R, Tomicek P, Roman M, Horacek J. [Time profile of serum THC levels in occasional and chronic marihuana smokers

after acute drug use—implication for driving motor vehicles]. *Soud Lek* 2014;**59**:2–6.

Battista N, Bari M, Maccarrone M. Endocannabinoids and reproductive events in health and disease. *Handb Exp Pharmacol* 2015;**231**: 341–365.

Battista N, Pasquariello N, Di Tommaso M, Maccarrone M. Interplay between endocannabinoids, steroids and cytokines in the control of human reproduction. *J Neuroendocrinol* 2008;**20**(Suppl 1):82–89.

Bottino C, Peserico A, Simone C, Caretti G. SMYD3: an oncogenic driver targeting epigenetic regulation and signaling pathways. *Cancers (Basel)* 2020;**12**:142.

Brents LK. Marijuana, the endocannabinoid system and the female reproductive system. *Yale J Biol Med* 2016;**89**:175–191.

Cavalcante RG, Sartor MA. annotatr: genomic regions in context. *Bioinformatics* 2017;**33**:2381–2383.

Cecconi S, Rossi G, Oddi S, Di Nisio V, Maccarrone M. Role of major endocannabinoid-binding receptors during mouse oocyte maturation. *Int J Mol Sci* 2019;**20**:2866.

Cylwa R, Kiełczewski K, Machnik M, Oleksiewicz U, Biecek P. KRAB ZNF explorer-the online tool for the exploration of the transcriptomic profiles of KRAB-ZNF factors in The Cancer Genome Atlas. *Bioinformatics* 2020;**36**:980–981.

Dobin A, Davis CA, Schlesinger F, Drenkow J, Zaleski C, Jha S, Batut P, Chaisson M, Gingeras TR. STAR: ultrafast universal RNA-seq aligner. *Bioinformatics* 2013;**29**:15–21.

ElSohly MA, Radwan MM, Gul W, Chandra S, Galal A. Phytochemistry of *Cannabis sativa* L. *Prog Chem Org Nat Prod* 2017; **103**:1–36.

Fonseca BM, Correia-Da-Silva G, Almada M, Costa MA, Teixeira NA. The endocannabinoid system in the postimplantation period: a role during decidualization and placentation. *Int J Endocrinol* 2013; **2013**:510540.

Fuchs Weizman N, Wyse BA, Szaraz P, Defer M, Jahangiri S, Librach CL. Cannabis alters epigenetic integrity and endocannabinoid signaling in the human follicular niche. *Hum Reprod* 2021;**36**: 1922–1931.

Herrera L, Ottolenghi C, Garcia-Ortiz JE, Pellegrini M, Manini F, Ko MS, Nagaraja R, Forabosco A, Schlessinger D. Mouse ovary developmental RNA and protein markers from gene expression profiling. *Dev Biol* 2005;**279**:271–290.

Howlett AC. The cannabinoid receptors. *Prostaglandins Other Lipid Mediat* 2002;**68-69**:619–631.

GTEx Consortium. The Genotype-Tissue Expression (GTEx) project. *Nat Genet* 2013;**45**:580–585.

Juan AM, Bartolomei MS. Evolving imprinting control regions: KRAB zinc fingers hold the key. *Genes Dev* 2019;**33**:1–3.

Jukic AM, Weinberg CR, Baird DD, Wilcox AJ. Lifestyle and reproductive factors associated with follicular phase length. *J Womens Health (Larchmt)* 2007;**16**:1340–1347.

Juknat A, Rimmerman N, Levy R, Vogel Z, Kozela E. Cannabidiol affects the expression of genes involved in zinc homeostasis in BV-2 microglial cells. *Neurochem Int* 2012;**61**:923–930.

Kesner AJ, Lovinger DM. Cannabis use, abuse, and withdrawal: cannabinergic mechanisms, clinical, and preclinical findings. *J Neurochem* 2021;**157**:1674–1696.

Klonoff-Cohen HS, Natarajan L, Chen RV. A prospective study of the effects of female and male marijuana use on in vitro fertilization (IVF) and gamete intrafallopian transfer (GIFT) outcomes. *Am J Obstet Gynecol* 2006;**194**:369–376.

Krueger F. Trim Galore! 2012. https://www.bioinformatics.babraham.ac.uk/projects/trim_galore/ (November 2020, date last accessed).

Krueger F, Andrews SR. Bismark: a flexible aligner and methylation caller for Bisulfite-Seq applications. *Bioinformatics* 2011;**27**: 1571–1572.

Leo C, Hsueh A. Ovarian Kaleidoscope Database. 2000.

Levin ED, Hawkey AB, Hall BJ, Cauley M, Slade S, Yazdani E, Kenou B, White H, Wells C, Rezvani AH *et al.* Paternal THC exposure in rats causes long-lasting neurobehavioral effects in the offspring. *Neurotoxicol Teratol* 2019;**74**:106806.

Li J, Zhang Q, Ge P, Zeng C, Lin F, Wang W, Zhao J. Is a prognostic lncRNA for patients with recurrent glioblastoma. *Dis Markers* 2020;**2020**:8888085.

Lopez-Cardona AP, Sanchez-Calabuig MJ, Beltran-Brena P, Agirregoitia N, Rizos D, Agirregoitia E, Gutierrez-Adan A. Exocannabinoids effect on *in vitro* bovine oocyte maturation via activation of AKT and ERK1/2. *Reproduction* 2016;**152**:603–612.

Love MI, Huber W, Anders S. Moderated estimation of fold change and dispersion for RNA-seq data with DESeq2. *Genome Biol* 2014; **15**:550.

Maccarrone M. Endocannabinoid signaling in female reproductive events: a potential therapeutic target? *Expert Opin Ther Targets* 2015;**19**:1423–1427.

Machnik M, Cylwa R, Kiełczewski K, Biecek P, Liloglou T, Mackiewicz A, Oleksiewicz U. The expression signature of cancer-associated KRAB-ZNF factors identified in TCGA pan-cancer transcriptomic data. *Mol Oncol* 2019;**13**:701–724.

Misner MJ, Taborek A, Dufour J, Sharifi L, Khokhar JY, Favetta LA. Effects of delta-9 tetrahydrocannabinol (THC) on oocyte competence and early embryonic development. *Front Toxicol* 2021;**3**:14.

Mueller BA, Daling JR, Weiss NS, Moore DE. Recreational drug use and the risk of primary infertility. *Epidemiology* 1990;**1**:195–200.

Murphy SK, Itchon-Ramos N, Visco Z, Huang Z, Grenier C, Schrott R, Acharya K, Boudreau M-H, Price TM, Raburn DJ *et al.* Cannabinoid exposure and altered DNA methylation in rat and human sperm. *Epigenetics* 2018;**13**:1208–1221.

Osborne AJ, Pearson JF, Noble AJ, Gemmell NJ, Horwood LJ, Boden JM, Benton MC, Macartney-Coxson DP, Kennedy MA. Genome-wide DNA methylation analysis of heavy cannabis exposure in a New Zealand longitudinal cohort. *Transl Psychiatry* 2020; **10**:114.

Pontis J, Planet E, Offner S, Turelli P, Duc J, Coudray A, Theunissen TW, Jaenisch R, Trono D. Hominoid-specific transposable elements and KZFPs facilitate human embryonic genome activation and control transcription in naive human ESCs. *Cell Stem Cell* 2019; **24**:724–735.e725.

Raudvere U, Kolberg L, Kuzmin I, Arak T, Adler P, Peterson H, Vilo J. g:Profiler: a web server for functional enrichment analysis and conversions of gene lists (2019 update). *Nucleic Acids Res* 2019;**47**: W191–W198.

Robinson MD, Oshlack A. A scaling normalization method for differential expression analysis of RNA-seq data. *Genome Biol* 2010;**11**: R25.

Rotermann M. *Analysis of Trends in the Prevalence of Cannabis Use and Related Metrics in Canada.* Ottawa, Ontario, Canada: Statistics Canada, 2019, 3–13.

Rowe HM, Jakobsson J, Mesnard D, Rougemont J, Reynard S, Aktas T, Maillard PV, Layard-Liesching H, Verp S, Marquis J et al. KAP1 controls endogenous retroviruses in embryonic stem cells. *Nature* 2010;**463**:237–240.

Sagvekar P, Kumar P, Mangoli V, Desai S, Mukherjee S. DNA methylome profiling of granulosa cells reveals altered methylation in genes regulating vital ovarian functions in polycystic ovary syndrome. *Clin Epigenetics* 2019;**11**:61.

Santoro M, Mirabella M, De Fino C, Bianco A, Lucchini M, Losavio F, Sabino A, Nociti V. Sativex® effects on promoter methylation and on CNR1/CNR2 expression in peripheral blood mononuclear cells of progressive multiple sclerosis patients. *J Neurol Sci* 2017;**379**:298–303.

Sassone-Corsi P. The cyclic AMP pathway. *Cold Spring Harb Perspect Biol* 2012;**4**:a011148.

Schrott R, Rajavel M, Acharya K, Huang Z, Acharya C, Hawkey A, Pippen E, Lyerly HK, Levin ED, Murphy SK. Sperm DNA methylation altered by THC and nicotine: vulnerability of neurodevelopmental genes with bivalent chromatin. *Sci Rep* 2020;**10**:16022.

Skopp G, Richter B, Potsch L. [Serum cannabinoid levels 24 to 48 hours after cannabis smoking]. *Arch Kriminol* 2003;**212**:83–95.

Smart R, Caulkins JP, Kilmer B, Davenport S, Midgette G. Variation in cannabis potency and prices in a newly legal market: evidence from 30 million cannabis sales in Washington state. *Addiction* 2017;**112**:2167–2177.

Sobocinska J, Molenda S, Machnik M, Oleksiewicz U. KRAB-ZFP transcriptional regulators acting as oncogenes and tumor suppressors: an overview. *Int J Mol Sci* 2021;**22**:2212.

Substance Abuse and Mental Health Services Administration (SAMHSA). *Results from the 2013 National Survey on Drug Use and Health: Summary of National Findings.* Rockville, MD, 2014.

Sun X, Dey SK. Endocannabinoid signaling in female reproduction. *ACS Chem Neurosci* 2012;**3**:349–355.

Szutorisz H, Hurd YL. Epigenetic effects of cannabis exposure. *Biol Psychiatry* 2016;**79**:586–594.

Takahashi N, Coluccio A, Thorball CW, Planet E, Shi H, Offner S, Turelli P, Imbeault M, Ferguson-Smith AC, Trono D. ZNF445 is a primary regulator of genomic imprinting. *Genes Dev* 2019;**33**:49–54.

Taylor AH, Ang C, Bell SC, Konje JC. The role of the endocannabinoid system in gametogenesis, implantation and early pregnancy. *Hum Reprod Update* 2007;**13**:501–513.

Treinen KA, Sneeden JL, Heindel JJ. Specific inhibition of FSH-stimulated cAMP accumulation by delta 9-tetrahydrocannabinol in cultured rat granulosa cells. *Toxicol Appl Pharmacol* 1993;**118**:53–57.

Volkow ND, Han B, Compton WM, McCance-Katz EF. Self-reported medical and nonmedical cannabis use among pregnant women in the United States. *JAMA* 2019;**322**:167–169.

Wang H, Xie H, Dey SK. Endocannabinoid signaling directs periimplantation events. *AAPS J* 2006;**8**:E425–432.

Watson CT, Szutorisz H, Garg P, Martin Q, Landry JA, Sharp AJ, Hurd YL. Genome-wide DNA methylation profiling reveals epigenetic changes in the rat nucleus accumbens associated with cross-generational effects of adolescent THC exposure. *Neuropsychopharmacology* 2015;**40**:2993–3005.

Xu J, Bao X, Peng Z, Wang L, Du L, Niu W, Sun Y. Comprehensive analysis of genome-wide DNA methylation across human polycystic ovary syndrome ovary granulosa cell. *Oncotarget* 2016;**7**:27899–27909.

Yang X, Bam M, Nagarkatti PS, Nagarkatti M. RNA-seq analysis of δ9-tetrahydrocannabinol-treated T cells reveals altered gene expression profiles that regulate immune response and cell proliferation. *J Biol Chem* 2016;**291**:15460–15472.

Yang X, Hegde VL, Rao R, Zhang J, Nagarkatti PS, Nagarkatti M. Histone modifications are associated with Δ9-tetrahydrocannabinol-mediated alterations in antigen-specific T cell responses. *J Biol Chem* 2014;**289**:18707–18718.

Yohn NL, Bartolomei MS, Blendy JA. Multigenerational and transgenerational inheritance of drug exposure: the effects of alcohol, opiates, cocaine, marijuana, and nicotine. *Prog Biophys Mol Biol* 2015;**118**:21–33.